Optics Letters

Impact of the boundary's sharpness on temporal reflection in dispersive media

Junchi Zhang,[1,*] W. R. Donaldson,[2] and Govind P. Agrawal[1,2]

[1]The Institute of Optics, University of Rochester, Rochester, New York 14627, USA
[2]Laboratory for Laser Energetics, University of Rochester, Rochester, New York 14623, USA
*Corresponding author: jzh156@ur.rochester.edu

Received 21 May 2021; revised 15 July 2021; accepted 17 July 2021; posted 19 July 2021 (Doc. ID 432180); published 13 August 2021

We investigate the impact of the finite rise time of a spatiotemporal boundary inside a dispersive medium used for reflection and refraction of optical pulses. We develop a matrix approach in the frequency domain for analyzing such spatiotemporal boundaries and use it to show that the frequency range over which reflection can occur is reduced as the rise time increases. We also show that total internal reflection can occur even for boundaries with long rise times. This feature suggests that spatiotemporal waveguides can be realized through cross-phase modulation even when pump pulses have relatively long rise and fall times.

https://doi.org/10.1364/OL.432180

Reflection of optical fields at a temporal boundary has attracted considerable attention in recent years [1–10]. Initially, a stationary boundary was considered [1,3], assuming that the refractive index changes suddenly at all spatial points at the same time. Such a temporal boundary is not easy to realize in practice, and it also ignores the dispersive nature of common optical media. A moving temporal boundary, called a spatiotemporal boundary, was considered in 2007 for a one-dimensional dispersionless medium, and Maxwell's equations were solved without any approximations [2]. Such a boundary was also used in Ref. [4] to study the temporal reflection of optical pulses inside a dispersive waveguide such as an optical fiber. A moving spatiotemporal boundary can be realized in experiments by using the nonlinear phenomenon of cross-phase modulation [11] induced by a pump pulse [6], or by applying a microwave pulse to a traveling-wave phase modulator.

In past studies, the moving spatiotemporal boundary was assumed to be infinitely sharp such that the refractive index changes instantaneously at its location. In practice, any boundary will have a finite rise time. One expects the results obtained for a sharp boundary to remain valid as long as the rise time is much shorter than other time scales of interest (such as the width of the pulse being reflected at the boundary). However, it is not known how the results obtained for a sharp boundary needs to be modified when the rise time of a spatiotemporal boundary is not negligible.

In this work, we investigate the impact of the finite rise time of a spatiotemporal boundary on the phenomena of temporal reflection and refraction. We employ a super-Gaussian function to model variations in the rise time of a boundary in terms of two controllable parameters. We divide the boundary region into multiple short-duration sections and develop a transfer-matrix approach in the frequency domain to study how the frequency of a specific plane-wave component changes as this plane wave passes from one section to the next. We discuss how this approach allows us to calculate the reflectivity spectrum for any spatiotemporal boundary with an arbitrary rise time. Our results show that the frequency range over which temporal reflection can occur is reduced as the rise time increases. They also show that total internal reflection (TIR) is not affected by the finite rise time of the boundary and can occur even for shallow boundaries (with a long rise time), as long as the change in the refractive index across it exceeds a certain amount. We verify these predictions through numerical simulations of short optical pulses propagating inside an optical fiber.

We consider a pulsed beam propagating inside a single-mode waveguide (such as an optical fiber) such that it maintains its spatial shape and size. In this situation, the electric field associated with this pulse can be written in the form

$$\mathbf{E}(\mathbf{r}, t') = \hat{\boldsymbol{e}} F(x, y) A(z, t') \exp[i(\beta_0 z - \omega_0 t')], \tag{1}$$

where $\hat{\boldsymbol{e}}$ is the polarization unit vector, $F(x, y)$ is the transverse spatial profile of the beam, and $A(z, t')$ is its slowly varying amplitude $A(z, t')$. Note that here t' is the time in laboratory frame. The field's rapidly varying part is assumed to oscillate at a reference frequency ω_0, and β_0 is the propagation constant at this frequency. At other frequencies present within the pulse's spectrum, the propagation constant can be expanded in Taylor series around ω_0 as [11]

$$\beta(\omega) = \beta_0 + \beta_1(\omega - \omega_0) + \frac{1}{2}\beta_2(\omega - \omega_0)^2, \tag{2}$$

provided that the spectrum of the incident pulse is narrow enough to make the higher-order terms negligible. Here, $\beta_1 = 1/v_g$ is related to the group velocity, and β_2 accounts for the group-velocity dispersion (GVD).

We assume that a spatiotemporal boundary, moving at the speed V_B, has been created inside the dispersive medium using a suitable technique (e.g., cross-phase modulation through a pump pulse) so that the refractive index of the medium differs by a small amount Δn on the two sides of this boundary. The problem is simplified by working in a frame in which the boundary is

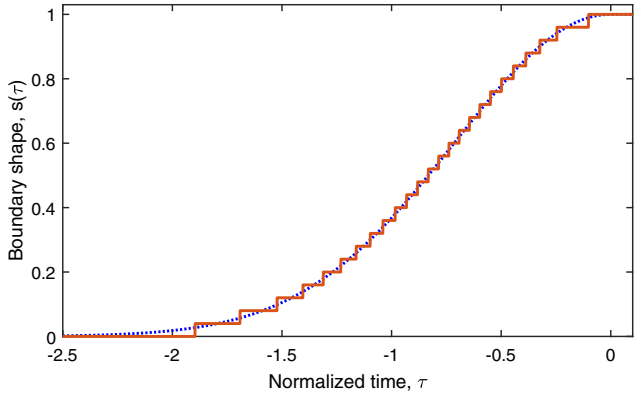

Fig. 1. Staircase approximation used to model a spatiotemporal boundary with a finite rise time. The step size is exaggerated for better visualization.

stationary. Introducing the reduced time $t = t' - z/V_B$ in this frame, the propagation of the pulse is governed by [4]

$$\frac{\partial A}{\partial z} + \Delta\beta_1 \frac{\partial A}{\partial t} + i\frac{\beta_2}{2}\frac{\partial^2 A}{\partial t^2} = i\beta_B s(t) A, \tag{3}$$

where $\Delta\beta_1 = \beta_1 - 1/V_B$, $\beta_B = (\omega_0/c)\Delta n$, and $s(t)$ governs the shape of the boundary with values in the range of zero to one. A spatiotemporal boundary becomes purely temporal in this frame, and we refer to the reflection on this boundary as temporal reflection. In most previous studies on temporal reflection, $s(t)$ was taken to be a step function of the form $h(t - T_B)$, assuming an infinitely sharp boundary located at $t = T_B$. In this work, we consider boundaries with a finite rise time T_r set by the functional form of $s(t)$ (see Fig. 1). For the present, we leave $s(t)$ unspecified and only note that its value rises from zero to one over a finite duration related to the rise time of the boundary. In general, one can solve Eq. (3) numerically, but such an approach provides little physical insight.

For a sharp boundary with $T_r = 0$, it is known that a pulse splits into two parts after it arrives at the boundary, which can be identified as the reflected and transmitted parts [4]. Their spectra are shifted from the spectrum of the incident pulse in such a way that the reflected part never crosses the boundary. It appears to move backward in the moving frame, even though it just moves slower compared to the incident pulse. We have recently developed an analytic, frequency-domain approach that allows us to calculate the frequency shifts, as well as the reflection and transmission coefficients as a function of the incident frequency [10]. We extend this approach to temporal boundaries of arbitrary shapes by making a reasonable approximation. As shown in Fig. 1, we divide the boundary region into N segments, each of finite duration such that $s(t)$ can be treated as a constant inside it. In other words, we replace the actual shape of the boundary with a staircase. This can be done for a boundary of any shape if we make N large enough that $s(t)$ does not vary much inside each segment. As we discuss next, we can use a transfer-matrix approach to move from one segment to the next, while employing our sharp-boundary results for each segment. Our approach is similar to that used for calculating the reflectivity of a stack of multiple dielectric layers [12]. The main difference is that we deal with temporal boundaries, in place of the spatial interfaces associated with the dielectric layers. We note that Eq. (3) is based on the slowly varying envelope approximation (SVEA) and requires pulses to be much wider than a single optical cycle. The error induced by SVEA has been discussed in Ref. [2].

Consider one spectral component of the pulse before the first segment with the frequency $\omega = \omega_0 + \delta_0$. It propagates as a plane wave $A_0 e^{i(Kz - \delta_0 t)}$. It follows from Eq. (3) that $K = \Delta\beta_1\delta_0 + \beta_2\delta_0^2/2$. As this plane wave traverses the boundary region, its frequency changes from one segment to the next. As K remains the same because of momentum conservation [4], only two plane waves exist in each section, but their frequencies change from one section to the next. One of these waves produces a reflected wave at a shifted frequency, and the other leads a transmitted wave. In the nth segment, where $s(t) = s_n$ is a constant, the two frequencies satisfy the dispersion relation

$$K = \beta_B s_n + \Delta\beta_1\delta_n + \frac{1}{2}\beta_2\delta_n^2. \tag{4}$$

We denote the two solutions of this quadratic equation as $\delta_{n\pm}$ and write the superposition of two plane waves as

$$A(z, t) = A_{n+} e^{i(Kz - \delta_{n+} t)} + A_{n-} e^{i(Kz - \delta_{n-} t)}. \tag{5}$$

Using this form, we can traverse the entire boundary region while keeping track of the frequency shifts in each segment.

To find the transfer matrix between two adjacent segments, let $\delta_\pm$ denote the frequency shifts on the left side and $\delta'_\pm$ on the right side. Using the boundary conditions that both A and its derivative $\partial A/\partial t$ should be continuous across the interface separating the two segments, we obtain

$$A_+ + A_- = A'_+ + A'_-, \tag{6}$$

$$\delta_+ A_+ + \delta_- A_- = \delta'_+ A'_+ + \delta'_- A'_-. \tag{7}$$

These equations can be written in the matrix form

$$\begin{pmatrix} A_+ \\ A_- \end{pmatrix} = \frac{1}{\tau}\begin{pmatrix} 1 & \rho \\ \rho & 1 \end{pmatrix}\begin{pmatrix} A'_+ \\ A'_- \end{pmatrix}, \tag{8}$$

where ρ and τ are, respectively, the reflection and transmission coefficients defined as

$$\rho = \frac{\delta_+ - \delta'_+}{\delta'_+ - \delta_-}, \qquad \tau = \frac{\delta_+ - \delta_-}{\delta'_+ - \delta_-}. \tag{9}$$

As ρ and τ are different for each section, we define the transfer matrix of the nth section as

$$T_n = \frac{1}{\tau_n}\begin{pmatrix} 1 & \rho_n \\ \rho_n & 1 \end{pmatrix}. \tag{10}$$

Within the nth section, two plane waves acquire time-dependent phase shifts. These can be included through a diagonal propagation matrix:

$$P_n = \begin{pmatrix} e^{i\delta_{n+}(t_{n+1} - t_n)} & 0 \\ 0 & e^{i\delta_{n-}(t_{n+1} - t_n)} \end{pmatrix}. \tag{11}$$

We use the transfer and propagation matrices to cross all segments, starting from the far end of the last segment. The resulting matrix of the entire spatiotemporal boundary is the product of $2N + 1$ matrices such that

$$M = \left(\prod_{n=1}^{N} T_n P_n\right) T_{n+1}. \tag{12}$$

In terms of the four elements of this matrix, the incident, reflected, and transmitted waves are related as

$$\begin{pmatrix} A_{in} \\ A_R \end{pmatrix} = \begin{pmatrix} M_{11} & M_{12} \\ M_{21} & M_{22} \end{pmatrix} \begin{pmatrix} A_T \\ 0 \end{pmatrix}. \tag{13}$$

It follows that the reflectivity and transmissivity of a spatiotemporal boundary are given by

$$R = |M_{21}/M_{11}|^2, \quad \mathcal{T} = |1/M_{11}|^2. \tag{14}$$

One simple way to consider boundaries with different rise times is to employ a specific shape controlled by the super-Gaussian function:

$$s(t) = \begin{cases} \exp[-((t - T_B)/T_0)^{2m}], & \text{for } t < T_B, \\ 1, & \text{for } t \geq T_B, \end{cases} \tag{15}$$

such that $s = 1$ at the boundary location $t = T_B$. The parameters T_0 controls the duration of the boundary, while m governs its sharpness. Increasing m makes the boundary sharper. If we use the engineering definition of the rise time and define T_r as the time it takes for $s(t)$ to increase from 10% to 90% of its final value, we obtain

$$T_r = T_0[(-\ln 0.1)^{1/2m} - (-\ln 0.9)^{1/2m}]. \tag{16}$$

We have found it useful to normalize β_B using its minimum value required for temporal TIR to occur. As discussed in Ref. [4], for a sharp boundary, TIR occurs when $\beta_B > (\Delta\beta_1 + \beta_2\delta_0)^2/(2\beta_2)$. We normalize β_B as $B = 2\beta_B\beta_2/(\Delta\beta_1 + \beta_2\delta_0)^2$. Physically, B represents the value of the index change relative to the value required for TIR to occur. We also normalize T_0 as $\tau_0 = |(\Delta\beta_1 + \beta_2\delta_0)/\beta_2|T_0$. Note that when normalizing, we used the quantity $\Delta\beta_1 + \beta_2\delta_0$. This is the effective $\Delta\beta_1$ of the incident wave of frequency $\omega_0 + \delta_0$. As the frequency shifts, the group-velocity mismatch between the incident wave and the moving boundary changes, and the reflectivity of the moving boundary changes. We have found that the reflectivity of a spatiotemporal boundary depends only on three dimensionless parameters: B, τ_0, m. We calculate its value numerically by dividing the boundary into a large number of segments (see Fig. 1) such that B differs at most by 0.005 between two neighboring segments.

To discuss the dependence of reflectivity on the rise time of a spatiotemporal boundary, we fix the input frequency at $\omega = \omega_0$ and set $\delta_0 = 0$. Figure 2(a) shows the reflectivity as a function of τ_0 for several values of m using $B = 0.98$, a value just below the TIR threshold of $B = 1$. In all cases, R decreases monotonically as the boundary's duration increases, but the rate of decrease depends on the rise time T_r. As T_r is reduced for larger values of m [see Eq. (16)], R remains relatively large over a wider range of τ_0. This feature shows that sharpness of the boundary plays an important role even when τ_0 is not small.

The dependence of reflectivity on the parameter B is even more critical because TIR can occur for $B \geq 1$. Figure 2(b) shows R as a function of B for several combinations of $\tau_0 = 1$ (solid lines) and $\tau_0 = 5$ (dashed lines). In each case, the rise time is reduced by changing $m = 1$ to $m = 3$. The most important feature here is that reflectivity becomes 100% when $B > 1$, regardless of the boundary's duration and shape. This means that the TIR occurs even for boundaries with a relatively long rise time, provided the index change across the boundary is large enough to ensure $B > 1$.

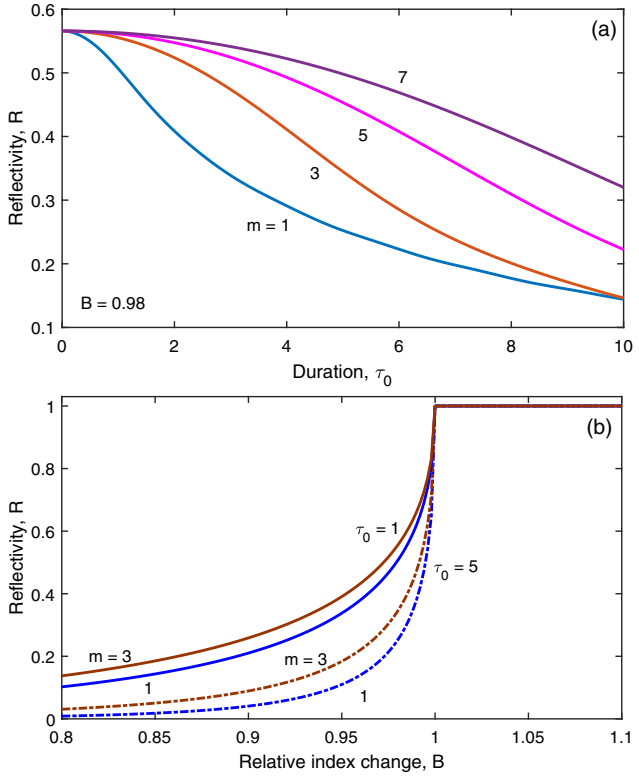

Fig. 2. (a) Reflectivity plotted as a function of τ_0 for several values of m using $B = 0.98$. (b) Reflectivity plotted as a function of B for $\tau_0 = 1$ (solid lines) and $\tau_0 = 5$ (dashed lines) with $m = 1$ and 3.

Another feature of Fig. 2(b) is that R decreases rapidly as B is reduced below one, and the decrease becomes more rapid for boundaries with longer durations. For example, when $\tau_0 = 5$ and $B = 0.9$, the reflectivity is only 4% for $m = 1$ (and 8.4% for $m = 3$). For even longer boundary durations, R becomes close to zero as soon as B is reduced below one, i.e., the reflectivity becomes a step function of B for long boundary durations. For such boundaries, an incident wave will not experience any reflection until the index change becomes large enough to make $B \geq 1$. At that point, the pulse undergoes TIR and is completely reflected.

The preceding discussion applies to one spectral component of a pulse at the frequency ω_0. We also need to consider the frequency dependence of the reflectivity. For this purpose, we choose $\Delta\beta_1 = 0.1$ ps/m, $\beta_2 = 0.005$ ps^2/m, and $\beta_B = 1.2$ m^{-1}. The last value corresponds to an index change of about 3×10^{-7} across the spatiotemporal boundary at wavelengths near 1 μm. Its use results in $B = 1.2$, indicating that the index change is large enough for TIR to occur in some frequency range. Figure 3 compares the reflectivity spectrum of a sharp boundary (dashed curve) with that of three boundaries with different rise times ($m = 1$, 5, and 10) using $T_0 = 0.5$ ps for the boundary's duration.

As seen in Fig. 3, TIR occurs for Δf values below 0.3 THz. The reason it ceases to occur for larger values Δf is related to a larger speed mismatch of the wave relative to the moving boundary. As Δf increases beyond 0.3 THz, $\Delta\beta_1$ keeps increasing, which decreases the reflectivity further. The rate of decrease depends on the boundary's rise time, and it becomes more and

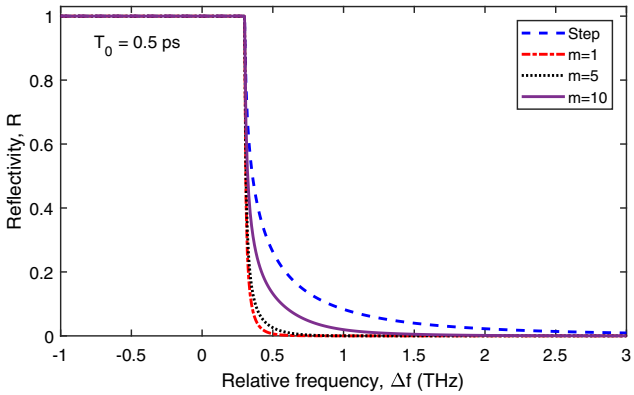

Fig. 3. Dependence of the reflectivity spectrum on the rise time of a spatiotemporal boundary (duration 0.5 ps) is shown using three values of m. Dashed curve shows for comparison the case of a step-function boundary.

more rapid as T_r increases (or m decreases). For a Gaussian-shaped boundary with $m = 1$, the reflectivity becomes nearly a step function of Δf. In practical terms, for such boundaries, a narrowband signal is either totally reflected or fully transmitted, depending on its frequency.

One may ask whether this behavior can occur for picosecond pulses whose spectrum is relatively wide. We use numerical simulations to show that it occurs for a 2-ps-wide Gaussian pulse launched into an optical fiber containing the moving boundary. More specifically, we solved Eq. (3) with the input $A_{\text{in}}(t) = \exp[-t^2/(2T_1^2)]$ and chose $T_1 = 2$ ps. We used the same values as in Fig. 3 for parameters $\Delta\beta_1$ and β_2. The spatiotemporal boundary had a Gaussian shape with $T_0 = 0.5$ ps, which corresponds to a normalized time of $\tau_0 = 10$. We considered two cases with $B = 0.95$ and $B = 1.05$. Recall that $B = 1$ corresponds to the TIR threshold.

Figure 4 shows the numerical results in these two cases by plotting the temporal evolution of the incident pulse over a 400-m-long fiber. In (a), most of the pulse energy crosses the boundary. In (b), nearly all energy is reflected because the index change across the boundary is larger by 10%, and exceeds the TIR threshold of $B = 1$. The reflection is not 100% because, even though the TIR condition is satisfied for the central frequency of the pulse, a portion of the pulse's spectrum lies outside the TIR region because of a relatively large bandwidth of the pulse. For wider pulses with smaller bandwidths, the change from full transmission to total reflection becomes more dramatic and exhibits a switch-like behavior in the sense that a relatively small change in the refractive index produces large changes in the transmitted energy of a probe pulse, when pump pulses are used to create a spatiotemporal boundary using the Kerr nonlinearity of an optical fiber.

In our past work, spatiotemporal boundaries formed inside a dispersive medium were taken to be infinitely sharp such that the refractive index changed instantaneously at its location. Here, we have investigated the impact of a finite rise time of the index change across the boundary on the spatiotemporal reflection and refraction of optical pulses. We developed a matrix approach in the frequency domain for analyzing such temporal

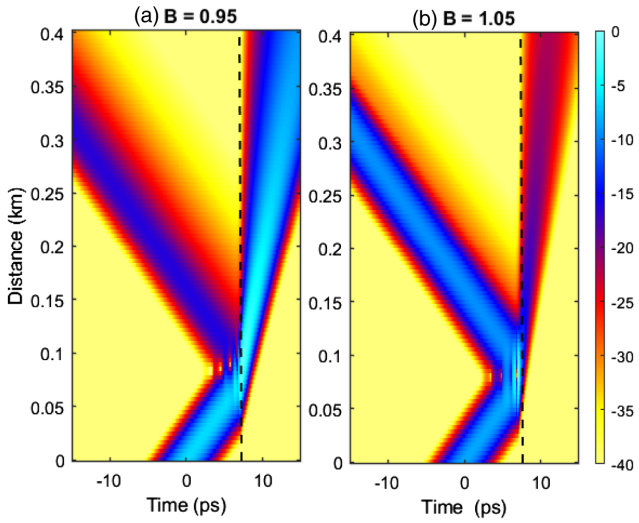

Fig. 4. Reflection and refraction of a 2-ps Gaussian pulse at a spatiotemporal boundary with 0.5-ps rise time ($m = 1$) for (a) $B = 0.95$ and (b) $B = 1.05$ ($B = 1$ is required for TIR to occur).

boundaries and used it to study the impact of a finite rise time. Our results show that the frequency range over which reflection occurs is reduced as the rise time increases. We also show that TIR can occur even for boundaries with a relatively long rise time. This feature suggests that temporal waveguides can be realized through cross-phase modulation even when pump pulses used in the experiment have relatively long rise and fall times.

Funding. National Science Foundation (ECCS-1933328).

Disclosures. The authors declare no conflicts of interest.

Data Availability. Data underlying the results presented in this paper are not publicly available at this time but may be obtained from the authors upon reasonable request.

REFERENCES

1. J. T. Mendonça and P. K. Shukla, Phys. Scr. **65**, 160 (2002).
2. F. Biancalana, A. Amann, A. V. Uskov, and E. P. O'Reilly, Phys. Rev. E **75**, 046607 (2007).
3. Y. Xiao, D. N. Maywar, and G. P. Agrawal, Opt. Lett. **39**, 574 (2014).
4. B. W. Plansinis, W. R. Donaldson, and G. P. Agrawal, Phys. Rev. Lett. **115**, 183901 (2015).
5. D. K. Kalluri, *Electromagnetics of Time Varying Complex Media: Frequency and Polarization Transformer*, 2nd ed. (CRC Press, 2016).
6. B. W. Plansinis, W. R. Donaldson, and G. P. Agrawal, J. Opt. Soc. Am. B **35**, 436 (2018).
7. C. Caloz and Z.-L. Deck-Léger, IEEE Trans. Anten. Propag. **68**, 1569 (2020).
8. D. Ramaccia, A. Toscano, and F. Bilotti, Opt. Lett. **45**, 5836 (2020).
9. V. Pacheco-Peña and N. Engheta, Optica **7**, 323 (2020).
10. J. Zhang, W. R. Donaldson, and G. P. Agrawal, J. Opt. Soc. Am. B **38**, 997 (2021).
11. G. P. Agrawal, *Nonlinear Fiber Optics*, 6th ed. (Academic, 2019).
12. S. J. Orfanidis, *Electromagnetic Waves and Antennas* (2016), Chap. 6.